C. R. Palevol 9 (2010) 73–81

Contents lists available at ScienceDirect

Comptes Rendus Palevol

www.sciencedirect.com

General palaeontology (Biostratigraphy)

# Upper Albian planktic foraminifera and radiolarian biostratigraphy (Nebeur – northern Tunisia)

## *Étude biostratigraphique des foraminifères planctoniques et des radiolaires de l'Albien supérieur (Nebeur – Tunisie septentrionale)*

Moez Ben Fadhel[a,*], Mohsen Layeb[b], Mohamed Ben Youssef[c]

[a] *Département des sciences de la terre, faculté des sciences de Bizerte, Soliman, Tunisia*
[b] *Institut supérieur arts et métiers, Siliana, Tunisia*
[c] *Département des géoressources, CERTE–Technopôle, Borj Cédria, Tunisia*

ARTICLE INFO

*Article history:*
Received 30 April 2008
Accepted after revision 18 January 2010
Available online 27 March 2010

Presented by Philippe Taquet

*Keywords:*
Radiolaria
Planktic foraminifera
Albian
Tunisia

*Mots clés :*
Radiolaires
Foraminifères planctoniques
Albien
Tunisie

ABSTRACT

Preliminary lithostratigraphic and biostratigraphic data recovered from Upper Albian pelagic successions of the Jebel Srassif area (Tunisian trough) reveal the presence of a moderately well preserved radiolarian fauna. This fauna is fossilized in blackshale beds of *Rotalipora subticinensis*, *R. ticinensis* and the lower part of the *R. appenninica* foraminifer zones. Thirty-five radiolarian morphotypes were identified. A correlation established with foraminifer planktic biochronology allows us to distinguish three radiolarian assemblages. The close association between organic-rich deposits and the radiolarian bloom can be interpreted as productivity proxy triggered by semi-enclosed basin configuration and an intensified upwelling currents provided by a possibly halokinetic-induced hydrothermalism.


RÉSUMÉ

L'étude lithostratigraphique et biostratigraphique des successions pélagiques de l'Albien supérieur de la région de Jebel Srassif (Sillon Tunisien) révèle l'existence d'une faune de radiolaires fossilisée dans des lits de *blackshales* dont l'âge est contrôlé par les zones de foraminifères *Rotalipora subticinensis*, *R. ticinensis* et la partie inférieure de la zone à *R. appenninica*. Trente-deux morphotypes de radiolaires ont été identifiés. Une corrélation établie avec ces biochronozones nous a permis de distinguer trois assemblages à radiolaires. La relation étroite entre les dépôts riches en matière organique et la prolifération des radiolaires peut être interprétée comme un proxy de productivité, en relation avec la configuration semi-fermée du bassin et un apport nutritif élevé, régis par un hydrothermalisme associé à la dynamique halocinétique.


## 1. Introduction

Albian radiolarian-rich deposits of the western Tethys realm were the subject of exhaustive biostratigraphic and paleoecologic studies (Bak, 1995; Erbacher, 1994; Gorican

* Corresponding author.
*E-mail address:* moez.benfadhel@yahoo.fr (M. Ben Fadhel).

1631-0683/$ – see front matter © 2010 Académie des sciences. Published by Elsevier Masson SAS. All rights reserved.
doi:10.1016/j.crpv.2010.01.002

and Smuc, 2004; Erbacher and Thurow, 1997; O'Dogherty, 1994; O'Dogherty and Guex, 2002). However, Middle Cretaceous pelagic successions of the North-African margins bearing radiolarian fauna have received less attention and have not been accurately studied, one notable exception being the contribution of Magné and Sigal (Magné and Sigal, 1956).

The aim of the present work is to establish a preliminary biostratigraphic analysis of the radiolarian fauna recovered from the Upper Albian pelagic successions of the Tunisian trough, and propose an interpretation for the depositional setting of the corresponding successions.

### 1.1. Material and methods

Due to the poor preservation and the calcitization of many radiolarian shells, identification of radiolarian taxa was difficult. In order to improve our results, specimens were extracted after repeated chemical treatments. The softer samples have been washed using standard techniques (soaked in hydrogen peroxide for few hours), then sieved (63 μm – 160 μm – 500 μm). Assemblages have been photographed with a Scanning Electronic Microscope (SEM) at the University of Claude-Bernard Lyon I, France. Abundance of radiolarian was assessed by counting the entire radiolarian content in each washed residue, as well as in thin sections.

### 1.2. Geologic setting

The Nebeur area is located in the northwestern extremity of the 'Dome Belt', a complex structure linked to Triassic extrusions and strike-slip faults, which characterize this area (Fig. 1). According to Chikhaoui et al., 1991 and Chikhaoui and Turki, 1996, the observed structural complexity was the result of the extensive tectonic movement, which led to the extrusion of Triassic evaporites during the Albian–Aptian period. Consequently, halokinetic and tilted blocks movements are responsible for the horst-and-graben architecture. The so-called 'tectonic corners', described by the previous authors, are induced by the reactivation of strike slip faults during the Tertiary compressive phase.

The Jebel Srassif section (Fig. 1) belongs to the subsiding basin of the Mellegue 'paleograben' (Chikhaoui et al., 1991) bordered by two structural highs: Koumine to the west and Nebeur to the east. Cretaceous successions (Fig. 2) are characterized by a thick pile of Aptian to Campanian pelagic sequences, which are affected by multiple non-depositional unconformities and condensed layers (Chikhaoui, 1988).

### 1.3. Description of the Jebel Srassif section

The Albian succession of Jebel Srassif (Fig. 2) is in contact with chaotic Triassic evaporites (gypsum, mineralized dolomite) and begins with ten meter-thick sandstone beds and silty shales alternations of Hameima formation yielding phosphate coprolites and abundant benthic microfauna. They are overlain by a blue to grey metric packstone bed (4 m) showing slumps figures and reworkings. The next unit, named Marne Inférieure, consists of thick grey-colored marly interval, which comprises of centimetric-thick grey limestone layers and reworked Triassic lithoclasts. This interval is overlain by a bioturbated and glauconite-rich limestone bed. It is overlain by alternations of grey-colored limestone and fissile black marl, which become thin-laminated and black-colored mudstones at the top. This unit is attributed to the Allam member (Burollet, 1956). The faunal content is rare, although some spherical radiolarian and belemnites were collected.

The Marne Moyenne consists of 130 meter-thick alternations of grey marl and limestone, which become dark and laminated at the top. A cyclic marl/limestone bundles (10 m) can be distinguished having an organic and radiolarian-rich mudstone texture. It is capped by a thick organic-rich limestone bed (20 m) characterized by bituminous odor and yellowish color in patina. This level corresponds to the Mouelha member (Burollet, 1956). The 40 meters of the top consist of an alternation of grey limestones and dark grey-ochre marls yielding septarian nodules characterizing the Defla member. They are overlain by a succession of lenticular limestone beds and grey marl of Azreg member (50 m).

## 2. Results and discussion

Three samples were selected, based on the good preservation of the faunal assemblages. Among 35 radiolarian morphotypes, only 23 species were figured. Biostratigraphic analysis of the fossil record and planktic foraminifer's zones (Fig. 3, and Plates 1 and 2) correlation allow us to distinguish the following three radiolarian assemblages:

1. The sample 37 has provided a diversified radiolarian fauna with the co-occurrence of *Dictyomitra montisserei* (SQUINABOL), *Obeliscoites perspicuus* (SQUINABOL), *Tubilustrium transmontanum* O'DOGHERTY, *Dictyomitra gracilis* (SQUINABOL), *Holocryptocanium barbui* DUMITRICA, *Stichomitra* aff. *navalis* O'DOGHERTY, *Cryptamphorella conara* (FOREMAN), *Torculum dengoi* (SCHMIDT-EFFING), *Stichomitra communis* SQUINABOL, *Torculum coronatum* (SQUINABOL), *Distylocapsa micropora* (SQUINABOL), *Patellula verteroensis* (PESSAGNO), *Godia concava* (LI & WU).

Bak (Arthur et al., 1990) established a radiolarian zonation (*H. barbui – H. geysersensis)* for the Albian–Cenomanian, based on the co-occurrence of *Holocryptocanium barbui* DUMITRICA, *Holocryptocanium geysersensis* PESSAGNO, *Novixitus weyli* SCHMIDT-EFFING, *Squinabollum fossile* (SQUINABOL), *Crymptamphorella macropora* DUMITRICA, *Hemicryptocapsa tuberosa* DUMITRICA. O'Dogherty (O'Dogherty, 1994) proposed a radiolarian zonation for the Albian based on Unitary Associations. He described for the Upper Albian to the base of the Cenomanian *Spoletoensis* zone divided into three radiolarian subzones: the *Romanus*, *Missilis* and *Anisa* subzones.

The first appearance of *B. breggiensis*, recorded within Upper Albian basal intervals, coincides with first appearance of radiolarian species *Tubilustrium transmontanum*

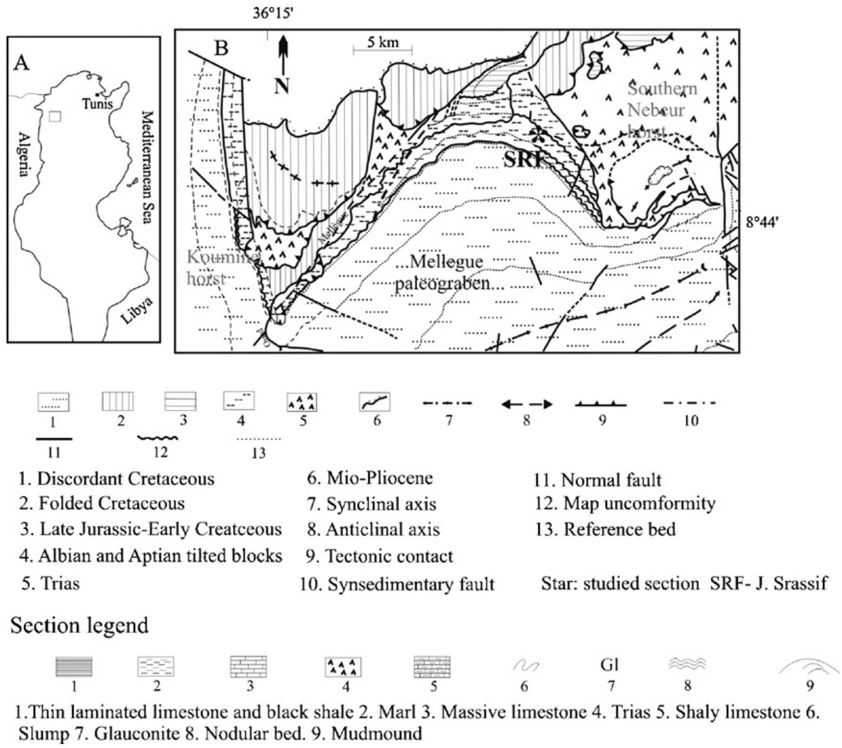


**Fig. 1.** Geological map of the Nebeur area (after Chikhaoui et al., 1991, modified).

**Fig. 1.** Carte géologique de la région de Nebeur (d'après Chikhaoui et al., 1991, modifiée).

O'DOGHERTY, which is confined with the upper part of the *Romanus* subzone (O'Dogherty, 1994). An assemblage containing *Stichomitra navalis* and *Torculum coronatum* was recorded also within this subzone. Babazadeh and de Wever (Babazadeh and de Wever, 2004) described a radiolarian assemblage yielding the co-occurrence of *Dictyomitra gracilis*, *Holocryptocanium barbui* and *Dictyomitra montisserei* and assigned it to Middle–Late Albian age. Nevertheless, the presence of *T. dengoi*, whose first appearance coincides with the *Missilis* – *Anisa* subzones boundary (O'Dogherty, 1994), allows rejuvenating the assemblage age.

2. Radiolarian assemblage recovered from sample 62 is highly diversified at the top of Mouelha blackshales. Likewise, it records an acme of species belonging to Hagiastridae and Cavaspongiidae taxa. This interval shows the co-occurrence of *Dispongotripus acutispinus* SQUINABOL, *Dactyliosphaera maxima* (PESSAGNO), *Pessagnobrachia* sp., *Cavaspongia euganea* (SQUINABOL), *Cryptamphorella conara* (FOREMAN), *Pessagnobrachia rara* (SQUINABOL), *Dorypyle communis* (SQUINABOL), *Pseudodictyomitra paronai* (ALIEV), *Pseudodictymitra* sp., *Torculum coronatum* (SQUINABOL), *Holocryptocanium tuberculatum* DUMITRICA, *Distylocapsa micropora* (SQUINABOL), *Obeliscoites perspicuuus* (SQUINABOL), *Dactyliosphaera acutispina* SQUINABOL, *Dictyomitra gracilis* (SQUINABOL), *Thanarla spoletoensis* O'DOGHERTY, *Dactyliosphaera lepta* (FOREMAN), *Patellula verteroensis* (PESSAGNO), *Savaryella novalensis* (SQUINABOL), *Savaryella quadra* (FOREMAN), *Pessagnobrachia fabianii* (SQUINABOL), *Stichomitra communis* SQUINABOL, *Holocryptocanium barbui* DUMITRICA, *Xitus* aff. *spicularius* (ALIEV), *Torculum coronatum* (SQUINABOL), *Crolanium* aff. *spineum* (PESSAGNO),

Samples recovered from the succession overlying the Mouelha blackshales show an assemblage composed of *Cryptamphorellla conara* Dumitrica, *Pessagnobrachia* sp., and *Thanarla spoletoensis* O'DOGHERTY, which correspond to the lower part of the *Appenninica* zone and the middle part of the *Anisa* subzone of O'Dogherty, 1994. Although the coexistence of *D. lepta*, *Stichomitra communis* and *Patellula verteroensis* is assigned to early Late Cenomanian age (Erbacher, 1998), this assemblage possibly characterizes the Late Albian taking into account the presence of *D. maxima* whose last occurrence is coeval with the base of *Anisa* subzone (O'Dogherty, 1994).

3. Sample 68 is characterized by the abundance of cryptocephalic nassellaria (*Holocryptocanium*). Moreover, we notice the first occurrence and bloom of *Mallanites triquetrus*. This interval shows the co-occurrence of *Xitus mclaughlini* (PESSAGNO), *Hexapyramis pantanelli* SQUINABOL, *Mallanites triquetrus* (SQUINABOL), *Thanarla spoletoensis* O'DOGHERTY, *Dictyomitra montisserei* (SQUINABOL), *Godia concava* (LI & WU), *Cryptamphorella conara* (FOREMAN), *Torculum coronatum* (SQUINABOL), *Cavaspongia euganea* (SQUINABOL), *Distylocapsa micropora* (SQUINABOL), *Dactyliosphaera maxima* (PESSAGNO), *Holocryptocanium barbui* DUMITRICA, *Dactyliodiscus longispinus* (SQUINABOL), *Dispongotripus acutispinus* SQUINABOL.

The radiolarian assemblages are characterized by high diversity rate thus making it possible to bring additional

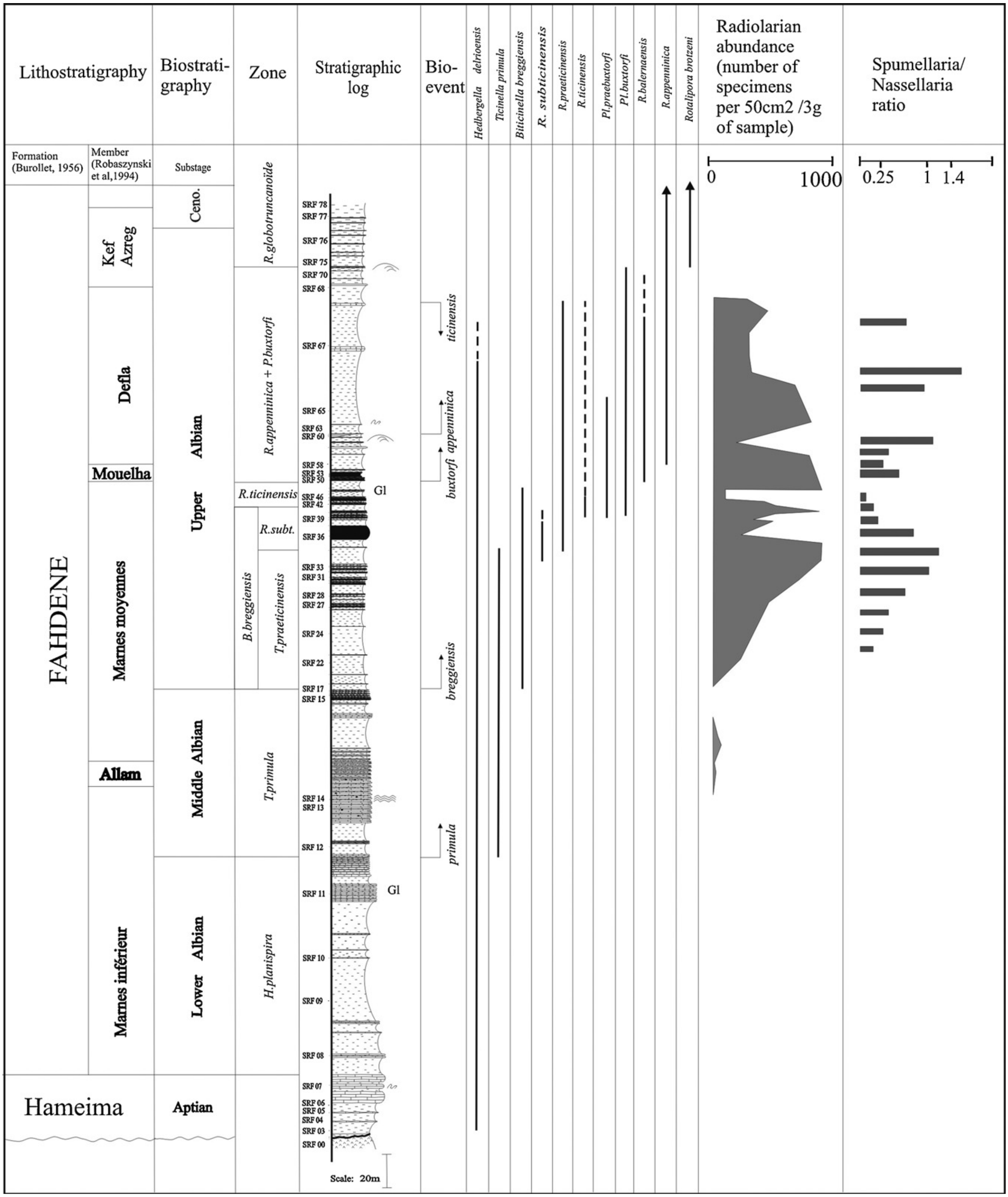


**Fig. 2.** Albian biostratigraphy of the Srassif section plotted against radiolarian abundance and nassellaria vs spumellaria ratio curves.

**Fig. 2.** Étude biostratigraphique de l'Albien de la coupe de J. Srassif, placée en face des courbes d'abondance des radiolaires et du rapport spumellaire/nassellaire.

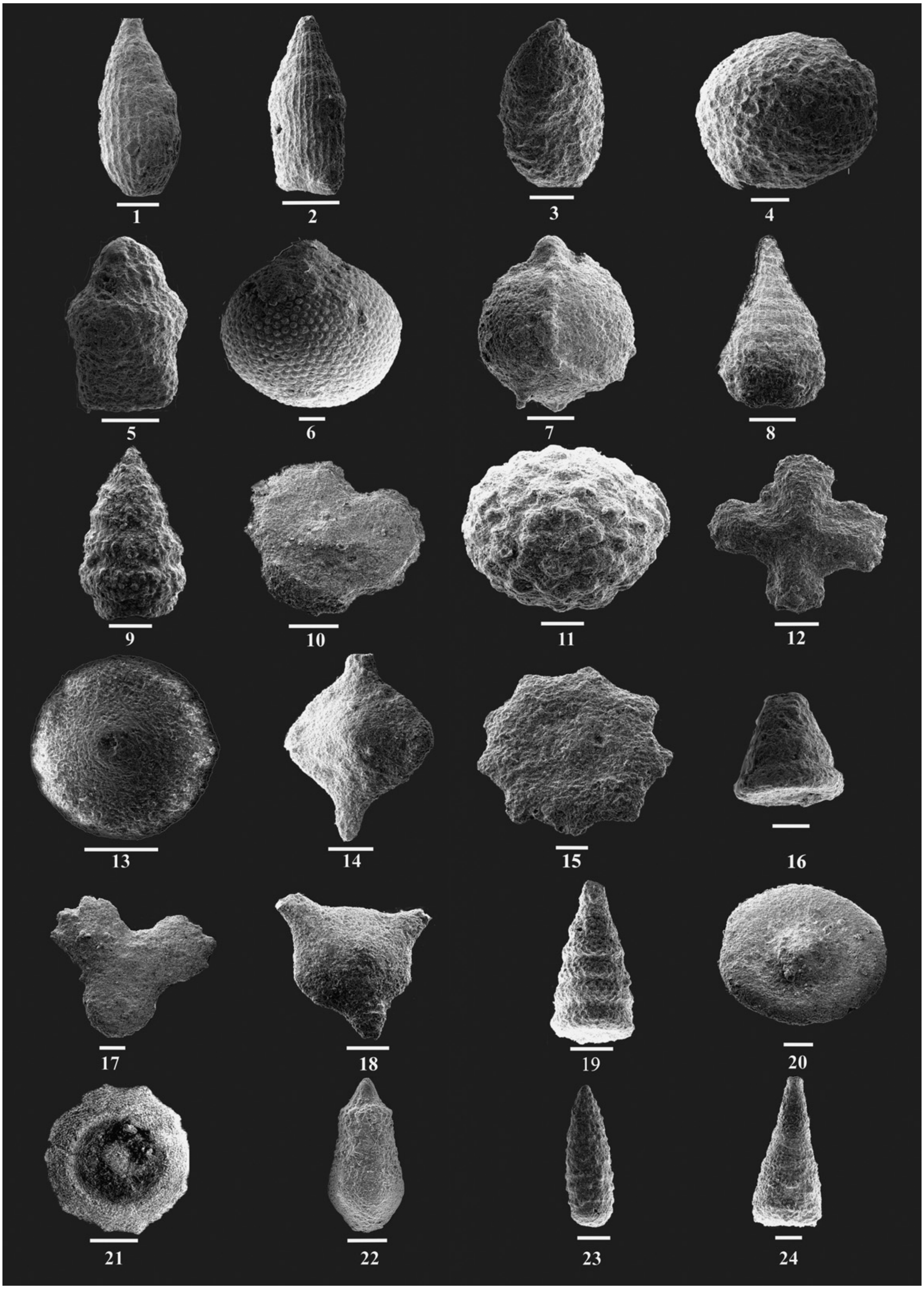
1
2
3
4
5
6
7
8
9
10
11
12
13
14
15
16
17
18
19
20
21
22
23
24

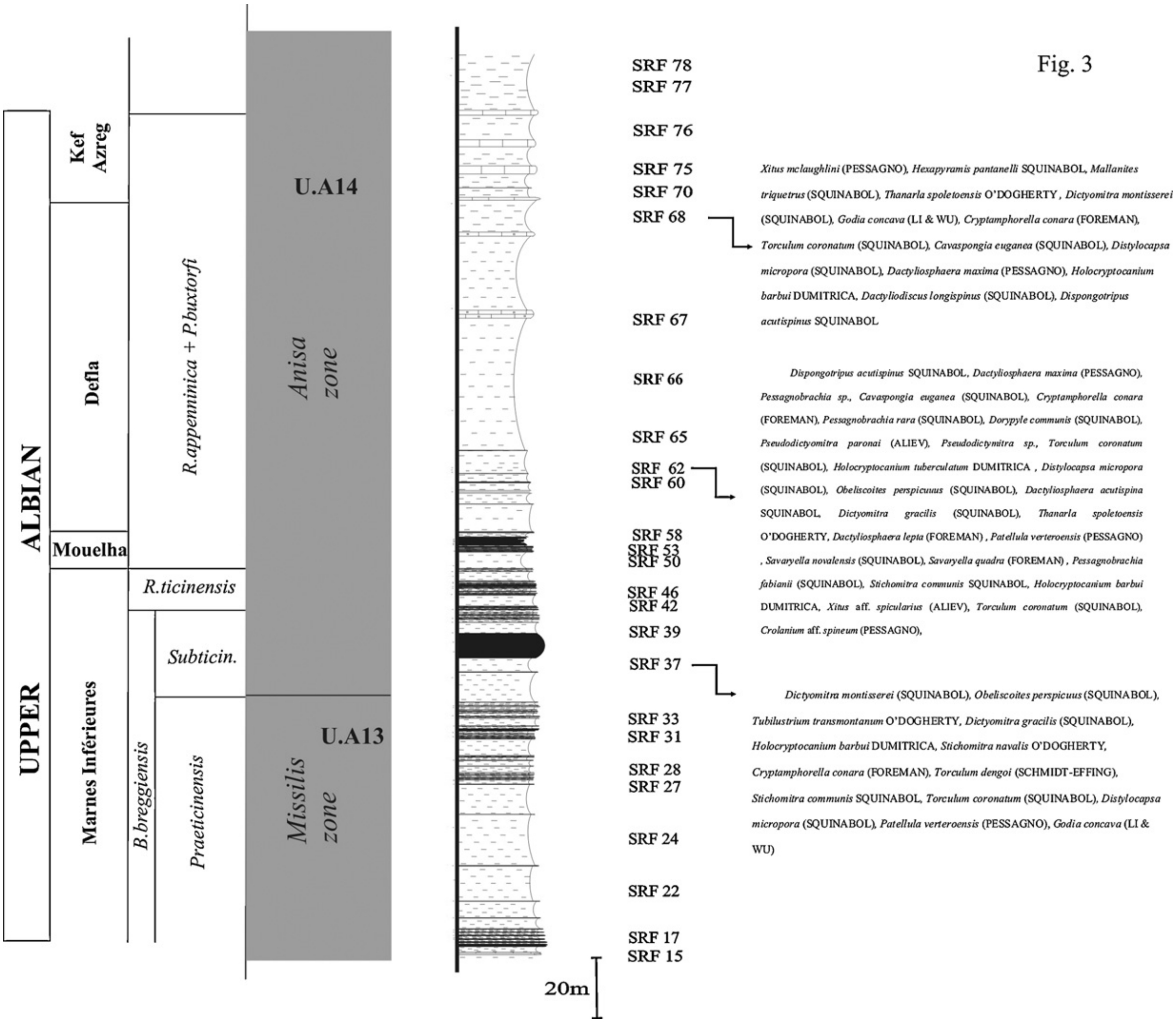


**Fig. 3.** Stratigraphic detail of the Srassif section with location of selected samples and radiolarian assemblages (radiolarian zones and Unitary Associations (UA) – grey area – according to O'Dogherty, 1994 and O'Dogherty and Guex, 2002).

**Fig. 3.** Détail de la stratigraphie de la coupe de J. Srassif et localisation des assemblages à radiolaires sélectionnés (les biozonations des radiolaires sont établies – surface grise – d'après la nomenclature de O'Dogherty, 1994 et O'Dogherty and Guex, 2002).

details about the J.Srassif pelagic successions age. It is worth noting in these assemblages, the abundance of cryptothoracic nassellaria *Holocryptocanium barbui*, which seems to be ubiquistic specie in these successions.

The correlation of these assemblages with biozonations based on Unitary Association established by O'Dogherty (1994) allows assigning these levels to the interval comprised between UAZ 13 and UAZ14 of Late Albian age.

**Plate 1.** Radiolarian.

**1** – *Dictyomitra gracilis* (SQUINABOL), scale bar: 50 μm, sample 62. **2** – *Dictyomitra montisserei* (SQUINABOL), scale bar: 50 μm, sample 68. **3** – *Tubilustrium transmontanum* O'DOGHERTY, scale bar: 50 μm, sample 37. **4** – *Holocryptocanium barbui* DUMITRICA, scale bar: 50 μm, sample 37. **5** – *Stichomitra* aff. *navalis* O'DOGHERTY, scale bar: 50 μm, sample 37. **6** – *Cryptamphorella conara* (FOREMAN), scale bar: 50 μm, sample 37. **7** – *Mallanites triquetrus* (SQUINABOL), scale bar: 100 μm, sample 68. **8** – *Dictyomitra gracilis* (SQUINABOL), scale bar: 100 μm, sample 62. **9** – *Xitus* aff. *spicularius* (ALIEV), scale bar: 100 μm, sample 62. **10** – *Dispongotripus acutispinus* SQUINABOL, scale bar: 100 μm, sample 62. **11** – *Holocryptocanium tuberculatum* DUMITRICA, scale bar: 50 μm, sample 62. **12** – *Savaryella quadra* DUMITRICA, scale bar: 100 μm, sample 62. **13** – *Patellula verteroensis* (PESSAGNO), scale bar: 150 μm, sample 37. **14** – *Dactyliosphaera lepta* (FOREMAN), scale bar: 50 μm, sample 62. **15** – *Dactyliodiscus longispinus* (SQUINABOL), scale bar: 50 μm, sample 68. **16** – *Torculum dengoi* (SCHMIDT-EFFING) Scale bar: 50 μm, sample: 37. **17** – *Pessagnobrachia* sp., scale bar: 100 μm, sample 62. **18** – *Cavaspongia euganea* (SQUINABOL), scale bar: 100 μm, sample 62. **19** – *Stichomitra communis* SQUINABOL, scale bar: 50 μm, sample 62. **20** – *Dactyliosphaera maxima* (PESSAGNO), scale bar: 100 μm, sample 62. **21** – *Godia concava* (LI & WU), scale bar: 100 μm, sample 37. **22** – *Torculum coronatum* (SQUINABOL), scale bar: 150 μm, sample 62. **23** – *Crolanium* aff. *spineum* (PESSAGNO), scale bar: 100 μm, sample 62. **24** – *Obeliscoites perspicuus* (SQUINABOL), scale bar: 100 μm, sample 62.

**Planche 1.** Radiolaires.

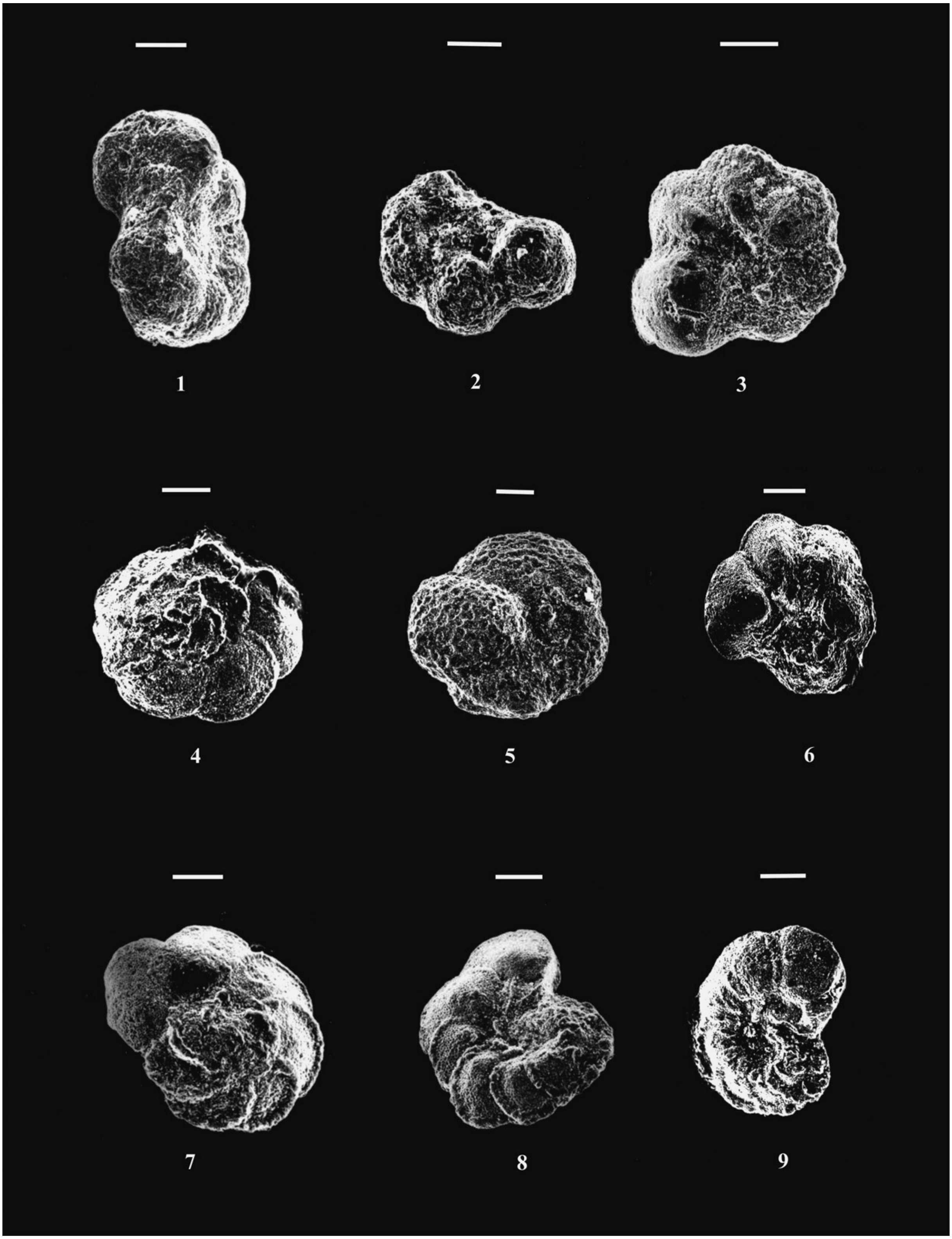

**Plate 2.** Planktic foraminifera (scale bar: 100 μm).
1 – *Biticinella breggiensis* (GANDOLFI), sample 37. 2 – *Ticinella primula* LUTERBACHER, sample 37. **3** – *Rotalipora subticinensis* (GANDOLFI), sample 37. **4** et **7** – *Rotalipora appenninica* (RENZ), sample 62. **5** – *Favusella washitensis* CARSEY, sample 37. **6** – *Rotalipora ticinensis* (GANDOLFI), sample 62. **8** et **9** – *Planomalina buxtorfi* (GANDOLFI), sample 68.
**Planche 2.** Foraminifères planctoniques (barre d'échelle : 100 μm).

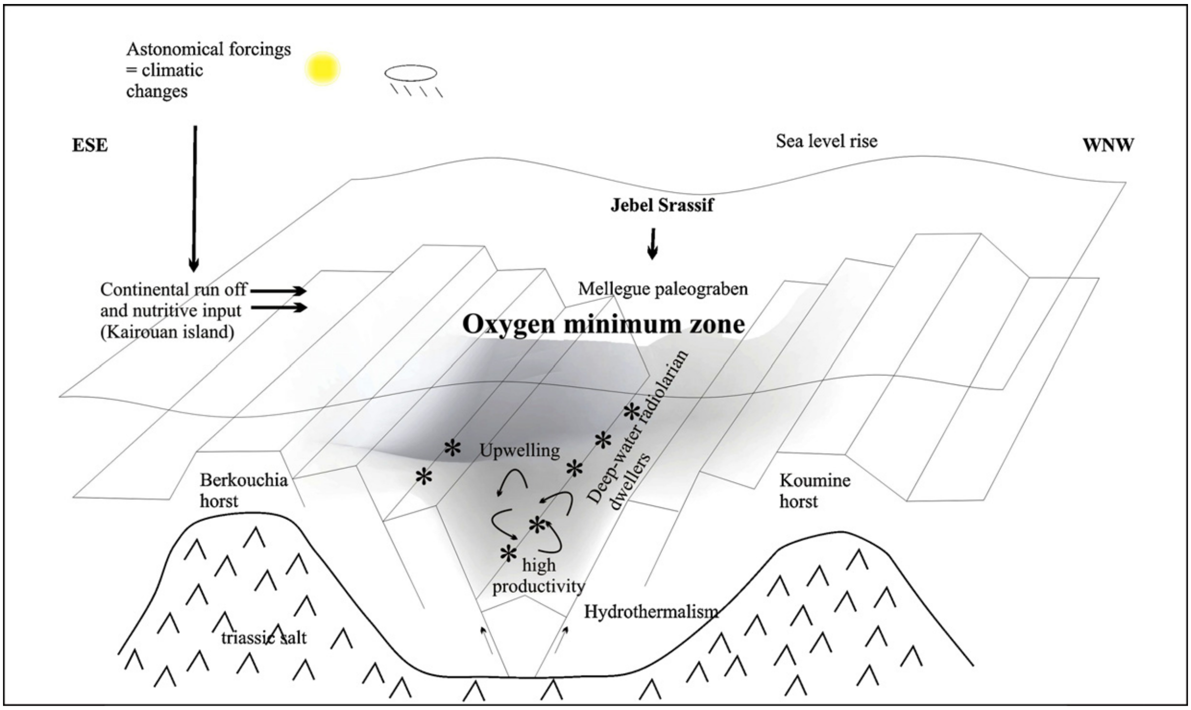


**Fig. 4.** Blackshales deposition model in the Srassif basin during the Albian.

**Fig. 4.** Modèle de dépôt des *blackshales* dans le bassin de Srassif durant l'Albien.

Radiolarian-bearing carbonate pelagic successions investigated in the Srassif section might not be considered as true radiolarite successions in the absence of true chert layers. The presence of interstratified limestone beds in the Jurassic radiolarian-bearing Jedidi Formation has been mentioned by Cordey et al., 2005 who emphasized the absence of true 'radiolarites' in Tunisia. They considered that such an occurrence of carbonates is indicative of a depocenter, although basinal, located above the CCD.

The peculiar co-occurrence of organic rich deposits (blackshales) and radiolarian blooms discovered in the studied section are to be outlined. Radiolarian-bearing deposition associated with blackshales has previously been observed within cherty limestones and/or bituminous deposits (Bogdanov and Vishnevskaya, 1992; Danelian et al., 2002; De Wever and Baudin, 1996; Erbacher et al., 1996; Musavu-Moussavou and Danelian, 2006; Robaszynski et al., 1993; Salvini and Marcucci Pesserini, 1998).

During the Mid-Cretaceous, organic rich-sediments were widely spread in Mediterranean Tethys basins as a result of Oceanic Anoxic Event (OAE) (Arthur et al., 1990; Jenkyns, 1980). Geochemical and biostratigraphic data recovered from Albian pelagic sequences of north-western Tunisia have yielded the records of OAE1b, OAE1c and OAE1d, which can be correlated with time-equivalent of northern Tethyan margins (Ben Fadhel et al., 2010). Basins configuration inherited from Early Jurassic rifting phase affecting the Tunisian platform (Boughdiri et al., 2007) were enhanced during the Mid-Cretaceous period by halokinetic dynamics, which have probably preserved basins geometry during post-rift period (Karakitsios, 1995). The resulting basins were filled then by organic-rich deposits, which were coeval with a sea level rise and hyper-silicious period characterizing the Tethys Realm during the Albian–Cenomanian (Racki and Cordey, 2000).

During the early Late Albian, the Srassif basin (Fig. 4) was the site of upwelling currents, an elevated radiolarian productivity triggered by silica enrichment, provided by halokinetic-induced hydrothermalism. This fact is suggested by depleted $O^{18}$ values obtained from authigenic carbonate nodules enclosed within black shale levels (unpublished data), which are indicative of carbonate precipitation derived from hot and meteoric hydrothermal waters (Hemadi, 1987; Layeb et al., in press). A high nutrient supply was provided by the continental runoff of the emerged area of Kairouan Island (M'rabet, 1981).

The decrease of S/N ratio (Fig. 2) can be interpreted as a result of a semi-enclosed basin structured with tilted blocs, leading to the widespread of the oxygen minimum zone (OMZ). Thus, assemblages dominated by nassellaria are indicative of deep-dwelling taxa, eutrophic conditions and vigorous upwelling regime (Premoli Silva et al., 1999). The Late Albian period is characterized by a more oxygenated and oligotrophic environment, following changes in basin configuration and the sudden collapse of the stratified water column, may be responsible for radiolarian diversification and the increase of S/N ratio.

Particular attention was paid to the interstratifications of radiolarian-rich layers into rhythmic limestone marls couplet, possibly reflecting a control of radiolarian productivity by Milankovitch cycle parameters variation. According to Ogg et al., 1992, such a trend is responsible for an abrupt change in tropical upwellings and periodically enhanced radiolarian production.

## 3. Conclusion

Radiolarians from Mid Cretaceous (Upper Albian) pelagic successions of the Tunisian trough are documented for the first time and used to propose age correlations. Further investigations are needed to enhance resolution of the biochronology as well as paleoecological interpretations, as faunal abundances may be related to taphonomic artefacts. However, it seems that the Srassif paleobasin recorded an anoxic environment and an associated biotic response, controlled by sea level rise and extensive tectonics, which prevailed during the Albian. Nutrient availability and radiolarian high productivity were possibly triggered by the continental runoff of the Kairouan Island, the upwelling currents and Si enrichment of the seawater probably related to halokinetic-induced hydrothermalism. Halokinetic dynamics were responsible for the preservation of basin configuration inherited from rifting phase. This could have favored the widespread of anoxic conditions and the deposition of organic-rich and radiolarian-bearing sediments.

## Acknowledgments

We very much appreciated valuable help by Professor Fabrice Cordey and his constructive comments and the improvement he brought to the manuscript. We are grateful to Professor Mourad Bedir, CERTE Director, for his support.

## References

Arthur, M.A., Jenkyns, H.C., Brumsack, H.J., Schlanger, S.O., Stratigraphy, 1990. Geochemistry, and paleoceanography of organic carbon-rich cretaceous sequences. In: Ginsburg, R., Beaudoin, B. (Eds.), Cretaceous resources events and rhythms. Background and plan for research. NATO ASI Series C: Mathematical and physical sciences. Kluwer Academic Publisher, Dordrecht, p. pp. 75-120.

Babazadeh, S.A, de Wever, P., 2004. Radiolarian Cretaceous age of Soulabest radiolarites in ophiolite suite of eastern Iran. Bull. Soc. Geol. France 175 (2), 121–129.

Bak, M., 1995. Mid Cretaceous Radiolaria from the Pieniny Klippen belt, Carpathians, Poland. Cretaceous Res. 16, 1–23.

Ben Fadhel M., Hedfi, A., Layeb M., Ben Youssef M. Albian oceanic anoxic events in northern Tunisia: biostratigraphic and geochemical insights, 5th International Conference on the Geology of the Tethys Realm (4–7 January 2010), South Valley University, Qena, Egypt, Abstract.

Bogdanov, N.A., Vishnevskaya, V.S., 1992. Influence of evolutionary changes in Radiolaria on sedimentary processes. Dokl. Akad. Nauk 324, 162–166 (in Russian).

Boughdiri, M., Cordey, F., Sallouhi, H., Maalaoui, K., Masrouhi, A., Soussi, M., 2007. Jurassic radiolarian-bearing series of Tunisia: biostratigraphy and significance to western Tethys correlations. Swiss J. Geosciences 100, 431–441.

Burollet, P.F., 1956. Contribution à l'étude stratigraphique de la Tunisie centrale. Ann. Mines Geol. 18, 350, Tunis.

Chikhaoui, M., 1988. Succession distension – Compression dans le sillon Tunisien. Secteur de Nebeur, El Kef (Tunisie centro – septentrional). Rôle des extrusions triasiques précoces lors de serrage alpin. Thèse 3e cycle, Université de Nice, France, p. 143.

Chikhaoui, M., Turki, M., 1996. Rôle et importance de la fracturation méridienne dans les déformations crétacée de la zone des diapirs (Tunisie septentrionale). J. Afr. Earth Sci. 21 (2), 271–280.

Chikhaoui, M., Turki, M., Delteil, M., 1991. Témoignage de la structurogenèse de la marge téthysienne en Tunisie, en Jurassique terminal – Crétacé (région d'El Kef Tunisie septentrional). Geol. Mediterraneenne XVIII (3), 125–133.

Cordey, F., Boughdiri, M., Sallouhi, H., 2005. First direct age determination from the Jurassic radiolarian-bearing siliceous series (Jedidi Formation) of north-western Tunisia. C. R. Geoscience 337, 777–785.

Danelian, T., Baudin, F., Gardin, F., Beltran, C., Masure, E., 2002. Early Aptian productivity increase as recorded in the Fourcade level of the Ionian zone of Greece. C. R. Geoscience 334, 1087–1093.

De Wever, P., Baudin, F., 1996. Paleogeography of radiolarite and organic-rich deposits in Mesozoic Tethys. Geol. Rundsch 85, 310–326.

Erbacher, J., 1994. Entwicklung und Palaeoozeanographie mittelkretazischer Radiolarien der westlichen Tethys (Italien) und des Nordatlatiks. Tuebinger Mikropalaeontologische Mitteilungen 12, 120.

Erbacher, J., 1998. Mid-Cretaceous radiolarians from the eastern equatorial Atlantic and their paleoceanography. In: Mascle, J., Lohmann, G.P., Moullade, M. (Eds.), Proceedings of the Ocean Program 159. Scientific Results, pp. 363–373.

Erbacher, J., Thurow, J., 1997. Influence of anoxic events on the evolution of Mid-Cretaceous radiolarians in the North Atlantic and western Tethys. Mar. Micropaleontology 30, 139–158.

Erbacher, J., Thurow, J., Littke, R., 1996. Evolution patterns of Radiolaria and organic matter variations: A new approach to identify sea-level changes in Mid-Cretaceous pelagic environments. Geology 24 (6), 499–502.

Gorican, S., Smuc, A., 2004. Albian Radiolaria and Cretaceous stratigraphy of Mt. Mangart (western Slovenia). Razprave 4. razreda SAZU (Ljubljana) 45 (3), 29–49.

Hemadi, H., 1987. Les silicates et carbonates authigènes des diapirs du Nord de la Tunisie, signification chimique et thermique. Thèse, Université de Paris-Sud, Orsay, 182 p.

Jenkyns, H.C., 1980. Cretaceous anoxic events: from continents to oceans. J. Geol. Soc. Lond. 137, 171–188.

Karakitsios, V., 1995. The influence of pre-existent structure and halokinesis on organic matter preservation and thrust system evolution in the Ionian Basin, northwest Greece. AAPG Bull. 79 (7), 960–980.

Layeb, M., Ben Fadhel, M., Ben Youssef, M. Bioconstructions carbonatées thrombolitiques et coralliennes dans l'Albien supérieur du Bassin-Fahdène (Tunisie centro-septentrionale) : stratigraphie, sédimentologie et genèse. Bull. Soc. geol. France (in press).

Magné, J., Sigal, J., 1956. Sur la position stratigraphique d'un niveau repère à radiolaires (Albien élevé et Vraconien) en Algérie. Bull. Soc. geol. France III fasc. (4-6), 345–353, 6e série.

M'rabet, A, 1981. Stratigraphie, sédimentation et diagenèse carbonatée des séries du Crétacé inférieur de Tunisie centrale. Thèse, Université de Paris-Sud, Orsay, 540 p.

Musavu-Moussavou, B., Danelian, T., 2006. The radiolarian biotic response to Oceanic Anoxic Event 2 in the southern part of the northern proto-Atlantic (Demerara Rise, ODP Leg 207). Rev Micropaleontology 49, 141–163.

O'Dogherty, L., 1994. Middle Cretaceous radiolaria biochronology and palaeontology from Umbria Apennines (central Italy) and Betic Cordillera (Spain). In: Mémoire de géologie, Lausanne, vol. 21, 413 p.

O'Dogherty, L., Guex, J., 2002. Rates and pattern of evolution among Cretaceous radiolarians: relations with global paleocenographic events. Micropaleontology 48 (1), 1–22.

Ogg, J.G., Karl, S.M., Behl, R.J., 1992. Jurassic through Early Cretaceous sedimentation history of the central equatorial Pacific and of sites 800 and 801. In: Proceedings ODP, Scientific Results 129, pp. 571–613.

Premoli Silva, I., Erba, E., Salvini, G., Locatelli, C., Verga, D., 1999. Biotic changes in Cretaceous oceanic anoxic events of the Tethys. J. Foraminiferal Res. 29 (4), 352–370.

Racki, G., Cordey, F., 2000. Radiolarian palaeoecology and radiolarites: is the present the key to the past? Earth-Science Rev. 52, 83–120.

Robaszynski, F., Caron, M., Amédro, F., Dupuis, Ch., Hardenbol, J., Gonzalez Donoso, J.M., et al., 1993. Le Cénomanien de la région de Kalaat Senan (Tunisie Centrale), litho-biostratigraphie et interprétation séquentielle. Rev. Paleobiologie 12, 351–505.

Salvini, G, Marcucci Pesserini, M., 1998. The radiolarian assemblages of the Bonarelli Horizon in the Umbria-Marches Apennines and southern Alps, Italy. Cretaceous Res. 19, 777–804.